Journal of Vibration Testing and System Dynamics 7(2) (2023) 169-186

Journal of Vibration Testing and System Dynamics

Journal homepage: https://lhscientificpublishing.com/Journals/JVTSD-Default.aspx

Impulse Response of an Elastic Rod with a Mass-damper-spring Termination

Siyuan Xing[1], Jian-Qiao Sun[2†]

[1] Department of Mechanical Engineering, California Polytechnic State University, San Luis Obispo, CA 93047, USA

[2] Department of Mechanical Engineering, School of Engineering, University of California, Merced, California, 95343, USA

Submission Info

Communicated by F. Z. Feng
Received 16 July 2022
Accepted 2 October 2022
Available online 1 April 2023

Keywords

Non-self-adjoint boundary value problems
Viscous boundary conditions
Particular solution method

Abstract

This paper investigates the impulse response of a longitudinally vibrating rod with a mass-damper-spring termination. The equations of motion of the system are derived using Lagrange's method. The vibration of the rod consists of rigid-body and elastic motions. The impulse response is predicted with a particular solution method which constructs the response as the summation of the solution satisfying homogeneous boundary conditions and a particular solution dealing with non-homogeneous boundary conditions. The particular solution method transforms the original partial differential equation to discrete dynamic systems represented in a state-space form. The transient and total impulse responses at selected locations on the rod are studied in detail. The vibration reduction of the rod by tuning the mass-damper-spring system is discussed with the help of root locus with respect to the mass, damping and stiffness parameters. The tuning of the mass-damper-spring system can change coupling between the rigid-body and elastic motions, which in turn can significantly affect the response of the rod. The method of particular solution is validated through the error analysis and response comparison of a rod with free-free boundary conditions.

1 Introduction

The dynamic response of structures with viscous boundary conditions has received considerable attention in recent years. Such systems have important applications in vibration isolation [1], sound absorption [2], boundary control [3]. For example, the sound propagation in a Helmholtz resonator can be modeled through the longitudinal vibration of a rod with a viscous termination [4]. The accurate prediction of the response in such a system is of great significance to the optimal design of the resonator. However, obtaining its response is an onerous task despite the simplicity of the system. This is because the viscous boundary condition will lead to a non-self-adjoint boundary value problem whose eigenfunctions are complex and non-orthogonal. The non-orthogonality of eigenfunctions will

†Corresponding author.
Email address: jqsun@ucmerced.edu

ISSN 2475-4811, eISSN 2475-482X/$-see front materials
DOI:10.5890/JVTSD.2023.06.005

complicate the solution procedure of the traditional method of eigenfunction expansion. This paper presents a particular solution method to deal with this issue.

Many efforts have been devoted to studying such structural systems with viscous boundary conditions since the late 1980s. Physically, the viscous boundary can be considered as the combination of absorptive and reflective boundaries. Based upon this idea, in 1988, Spiekermann and Radcliffe [4] investigated the acoustic response in a one-dimensional tube with a damped boundary by decomposing it into the summation of propagating and standing waves associated with absorptive and reflective boundaries. However, the total response from this approach may not satisfy the original boundary conditions. One year later, Singh [5] presented a method of complex eigenvalue analysis through a longitudinally vibrating rod fixed at one end and with a damped boundary condition at the other end. Following this work, Prater and Singh [6] developed a numerical algorithm to determine the complex eigenvalues and eigenfunctions in a beam structure with arbitrarily distributed viscous dampers. Around 2000, Gürgöze and collaborators [7–9] adopted this approach to study the complex modes of longitudinally vibrating rods with secondary systems in-span.

However, the eigenfunctions with viscous boundary conditions are non-orthogonal, which poses considerable difficulties in computing the time response with the traditional eigenfunction expansion method. In 1990, Hull et al [10] reported a technique that augments the spatial interval from $[0, L]$ to $[-L, L]$ in which orthogonal eigenmodes exist. Therefore, the modal expansion approach can be applied. Using the same method, Hull [11] obtained a closed-form solution of the longitudinal response of a bar with a viscous boundary condition. Alternatively, Jayachandran and Sun [12], inspired by the work on non-self-adjoint operators in the applied mathematical community [13–20], addressed the non-orthogonality of eigenfunctions by transforming the problem into a self-adjoint boundary value problem in a Hilbert space. The modal expansion in the Hilbert space was used to formulate the adaptive-passive control of a 1-D acoustic system. Based upon a similar idea, Oliveto et al [21] in 1997 developed a complex modal expansion method by defining new orthogonality conditions. Following this work, Svedholm et al [22] investigated the vibration of a damped beam with general boundary conditions under a moving load, and Alati et al [23] studied a one-dimensional rod with arbitrary viscous damping devices. In the early 2000s, Sorrentino et al [24, 25] proposed another complex modal expansion method using a state-space method in conjunction with a transfer matrix method. In 2013, Jovannovic [26] presented a novel approach that reconstructs the differential operator of equations of motion using a state-space form. In the state-space representation, a bi-orthogonal vector space can be defined, which permits a Fourier series representation of the solution. The methods based on Green's functions have also been used to predict the response of structures with viscous boundary conditions. In 2011, Jovannovic and Koshkin [27] investigated a longitudinally vibrating bar with dampers at two ends and in-span. They solved the Green's function of the system in the Laplace domain and used series expansion to approximate the inverse Laplace transformation of the Green's function. In 2016, Failla [28] presented the frequency response of beams and plane frames with external and internal viscoelastic dampers. This work adopted a generalized function approach that gives the closed-form solution of dynamic Green's functions. However, as pointed out in [2], the solution based on Green's functions can lead to significant error at boundaries.

Recently, there is a growing interest in railway-bridge dynamics with soil-structure interactions, due to the development of high-speed trains. Studies [29, 30] have shown that the bridge response can be considerably affected by soil medium and foundation type, which can be modeled as viscoelastic boundary conditions. In 2020, Hirzinger et al [31] performed the dynamical analysis of a mass-spring-damper terminated, damped beam subjected to a moving train represented by a mass-spring-damper system. Through the complex modal expansion, the structural dynamics with bridge-soil interaction is represented by ODEs in state space, coupled with a train subsystem. The dynamical response was then computed numerically. One year later, König et al [32] extended this model by considering a multiple degree-of-freedom train model including the body, two bogies, and four axles. In 2022, König et al [33] further studied the effect of geometric track irregularities. Meanwhile, Zangeneh et al [34] predicted the free vibration of a viscoelastically supported beam under a moving load using a lumped two-degree-of-freedom model. Qiao and Rahmatalla [35] proposed a method to identify the viscoelastic boundary conditions from the dynamic response of a beam subject to a moving loading using the complex modal analysis in conjunction with a pattern-search optimization method.

This study focuses on the impulse response of a 1-D longitudinally vibrating rod with a free end at left and a mass-damper-spring termination at right (see Fig.1). The boundary conditions permit the rigid-body motion of the rod that generates an instant response at the right end after impact. The consequence of this is that two waves, i.e. the impulse wave produced at the left end and the response wave generated by the termination at the right end, will propagate along the rod simultaneously and reflect at both ends. To authors' best knowledge, such dynamics due to impulsive loading and m-c-k termination is not well studied in the literature.

The goal of this research is to develop a data-driven approach to identify termination conditions in terms of the parameters m, c and k such that the response at the termination is minimized. To this end, an analytical predictor that can give accurate solutions inside the rod as well as at the termination is also of significance. Using the predictor, one can generate abundant training data in the parameter space without performing costly experiments or using computationally expensive finite element methods. This paper will pave the way for our following research on applying data-driven methods for the optimization of termination design in such a system.

Although extensive research has been conducted on the dynamic response of elastic rod with viscous boundary conditions, few experimental study of such a system has been performed, partly because of the difficulty to build a damper without the inertial and stiffness effect of the device. This paper explicitly investigates the effects of inertial, damping and stiffness on the impact response of the rod, and will provide a theoretical foundation for experimental studies in the future. Furthermore, the study of this paper can lead to creation of new configurations of the well-known Hopkinson bar experimental setup. As a consequence, new research topics and applications based on the Hopkinson bar with various terminations can be developed in the future.

This paper will proceed with the modeling of the system in Fig.1 using Lagrange's method. We will split the rigid-body and elastic motions from the rod response such that their interactions can be represented explicitly in the equations of motion. To solve for the impulse response of the system, we will apply a particular solution method that constructs the response as the summation of a series solution of homogeneous boundary value problem and a particular solution satisfying the non-homogeneous boundary condition. This method has been demonstrated (see [2, 36]) to be effective in predicting the response of vibration of linear and nonlinear continuous systems. Through this method, the original partial differential equation will be transformed into a discrete dynamic system represented in a state-space form, subject to the initial conditions generated by the impact loading. We will present impulse responses at specific locations on the rod. The solution can perfectly capture the dynamics of the system under the impact loading. We will then use the same approach to approximate the solution with a damped boundary condition. We will demonstrate the vibration reduction of the system with the help of root locus with respect to the mass-damper-spring parameters. Finally, we will validate the particular solution method by the error analysis and response comparison of a rod with free-free boundary conditions.

2 Mathematical model

A uniform elastic rod with a mass-damper-spring system attached to its right end is shown in Fig.1. The rod is at rest initially and excited by an impact loading applied to its free end. The displacement

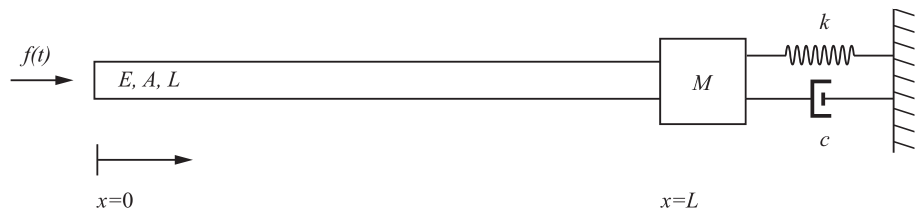

Fig. 1 A uniform elastic rod with a mass-damper-spring system at the right termination. An impact loading $f(t)$ is applied at the left free end. According to the convention in Structural Dynamics [37,38], x $(0 \leq x \leq L)$ is the material coordinate attached to the particle of the rod. All the displacements $u(x,t)$ and $u_M(t)$ are referenced to an inertial frame.

of the rod and mass are denoted by $u(x,t)$ and $u_M(t)$, respectively. Let $u(x,t) = u_r(t) + u_e(x,t)$ where $u_r(t)$ represents the rigid-body motion and $u_e(x,t)$ represents the elastic motion of the rod with non-zero frequency. It should be noted that the rigid-body motion $u_r(t)$ is a mode of rod response with zero frequency. Separation of the rigid and elastic motions only serves the purpose to streamline the programming later. At the right end, we have the continuity of displacement as $u_M(t) = u(L,t) = u_r(t) + u_e(L,t)$.

The kinetic and potential energies of the system including the inertial and stiffness elements at the boundary $x = L$ are given by

$$\begin{aligned} T &= \frac{1}{2}\int_0^L \rho A(\frac{\partial u}{\partial t})^2 dx + \frac{1}{2}M(\frac{du_M}{dt})^2 \\ &= \frac{1}{2}\rho A L \dot{u}_r^2 + \frac{1}{2}\rho A \int_0^L (2\dot{u}_r \frac{\partial u_e}{\partial t} + (\frac{\partial u_e}{\partial t})^2) dx \\ &\quad + \frac{1}{2}M(\dot{u}_r^2 + 2\dot{u}_r \dot{u}_e(L,t) + \dot{u}_e^2(L,t)) \end{aligned} \tag{1}$$

and

$$\begin{aligned} V &= \frac{1}{2}\int_0^L EA(\frac{\partial u}{\partial x})^2 dx + \frac{1}{2}k u_M^2 \\ &= \frac{1}{2}\int_0^L EA(\frac{\partial u_e}{\partial x})^2 dx + \frac{1}{2}k(u_r(t) + u_e(L,t))^2, \end{aligned} \tag{2}$$

where ρ, A, E and L are the density, cross-section area, Young's modulus, and length of the rod. M, c and k represent the mass, damping and stiffness at the termination.

It is assumed that the impact loading is applied to both the rigid-body and elastic motion. Therefore, the virtual work done by the impact loading over the virtual displacement $\delta u(x,t)$ and by the damper at $x = L$ is given by

$$\delta W = f_0 \delta(t) \delta u_r + \int_0^L \varepsilon f_0 \delta(x) \delta(t) \delta u_e(x,t) dx - c\dot{u}_M(\delta u_r + \delta u_e(L,t)), \tag{3}$$

where ε is an infinitesimal number used to remove the singularity introduced by the impact loading as $t \to 0$ and $x \to 0$.

The Hamilton's principle reads

$$\int_{t_1}^{t_2} (\delta L + \delta W) dt = 0, \tag{4}$$

where $L = T - V$. Substituting Eqs. (1), (2) and (3) into Eq. (4) and balancing the coefficients of variations yield the equations of motion

$$\begin{aligned}&(\rho AL+M)\ddot{u}_r+c\dot{u}_r+ku_r\\&+\rho A\int_0^L \frac{\partial^2 u_e}{\partial t^2}dx+M\ddot{u}_e(L,t)+c\dot{u}_e(L,t)+ku_e(L,t)=f_0\delta(t),\end{aligned}\tag{5}$$

$$\rho A(\ddot{u}_r+\frac{\partial^2 u_e}{\partial t^2})=\varepsilon f_0\delta(x)\delta(t)+EA\frac{\partial^2 u_e}{\partial x^2},\tag{6}$$

and boundary conditions

$$EA\frac{\partial u_e}{\partial x}(0,t)=0,\tag{7}$$

$$EA\frac{\partial u_e}{\partial x}(L,t)=-M(\ddot{u}_r+\ddot{u}_e(L,t))-c(\dot{u}_r+\dot{u}_e(L,t))-k(u_r+u_e(L,t)).\tag{8}$$

3 Method of particular solution

The rod vibration problem in Section 2 for the time $t \ge 0^+$ right after the impact loading can be recast as

$$\begin{aligned}&\rho AL\ddot{u}_r+M\ddot{u}_r+c\dot{u}_r+ku_r+\rho A\int_0^L \frac{\partial^2 u_e(x,t)}{\partial t^2}dx\\&+M\ddot{u}_e(L,t)+c\dot{u}_e(L,t)+ku_e(L,t)=0,\end{aligned}\tag{9}$$

$$c_p^2\frac{\partial^2 u_e}{\partial x^2}=\ddot{u}_r+\frac{\partial^2 u_e}{\partial t^2},\tag{10}$$

with boundary conditions

$$EA\frac{\partial u_e(0,t)}{\partial x}=0,\tag{11}$$

$$\begin{aligned}EA\frac{\partial u_e}{\partial x}(L,t)=&-M(\ddot{u}_r+\frac{\partial^2 u_e}{\partial t^2}(L,t))\\&-c(\dot{u}_r+\frac{\partial u_e}{\partial t}(L,t))-k(u_r+u_e(L,t)).\end{aligned}\tag{12}$$

The initial conditions can be obtained from the following,

$$\rho AL\dot{u}_r(0)+\rho A\int_0^L \frac{\partial u_e}{\partial t}(x,0)dx+M\left(\dot{u}_r(0)+\dot{u}_e(L,0)\right)=f_0,\tag{13}$$

$$c_p^2\frac{\partial u_e}{\partial x}(0,0)+\frac{1}{\rho A}f_0=\dot{u}_r(0)+\frac{\partial u_e}{\partial t}(0,0),\tag{14}$$

$$u_r(0)+u_e(x,0)=0,\ \text{with } 0\le x\le L,\tag{15}$$

$$\frac{\partial u_e}{\partial t}(x,0)=0,\ \text{with } 0< x\le L,\tag{16}$$

where $c_p = \sqrt{E/\rho}$ is the speed of the longitudinal stress wave traveling in the rod. Details on how to obtain these conditions can be found in the appendix.

We assume that the elastic motion consists of a homogeneous solution $u_h(x,t)$ and a particular solution $u_p(x,t)$ such that

$$u_e(x,t)=u_h(x,t)+u_p(x,t).\tag{17}$$

The particular solution $u_p(x,t)$ is constructed to satisfy the non-homogeneous boundary condition in Eq. (12). As a consequence, the homogeneous solution $u_h(x,t)$ only needs to satisfy homogenous boundary conditions, i.e. free-free boundary conditions. But, the governing equation for $u_h(x,t)$ becomes non-homogeneous. However, the boundary value problem to determine $u_h(x,t)$ is now self-adjoint. Therefore, the eigen-functions of this self-adjoint problem are the best choice to represent the solution $u_h(x,t)$ as shown below, together with a choice of the particular solution $u_p(x,t)$.

$$u_h(x,t) = \sum_{i=1}^{n} \phi_i(x) y_i(t), \tag{18}$$

$$u_p(x,t) = (\frac{x}{L})^m \alpha(t). \tag{19}$$

where $m > 1$ is an integer to be determined, $\phi_i(x)$ is the i-th elastic mode function of a rod with free-free boundary conditions such that

$$\int_0^L \phi_i(x)\phi_j(x)dx = \delta_{ij}. \tag{20}$$

It is noted that the rigid body mode of the free-free rod is not included in Eq. (18) for $u_h(x,t)$ because the rigid body motion $u_r(t)$ is already included in the total response $u(x,t)$ of the rod. Substitution of Eqs. (17) - (19) into the boundary condition at $x = L$ in Eq. (12) yields

$$\begin{aligned} &\sum_{i=1}^{n} \left[M\ddot{y}_i(t) + c\dot{y}_i(t) + ky_i(t)\right] \phi_i(L) + M\ddot{u}_r(t) + c\dot{u}_r(t) + ku_r(t) \\ &+ M\ddot{\alpha}(t) + c\dot{\alpha}(t) + (k + EAm/L)\alpha(t) = 0. \end{aligned} \tag{21}$$

It is noted that this boundary condition at $x = L$ does not contain the homogeneous part $u_h(x,t)$ of the elastic response. Instead, $u_h(x,t)$ satisfies free-free boundary conditions, as pointed out earlier.

Substitution of Eqs. (17) - (19) into Eq. (9) yields

$$\begin{aligned} &\rho AL\ddot{u}_r + [M\ddot{u}_r(t) + c\dot{u}_r(t) + ku_r(t)] + \rho A\bar{\phi}_0\ddot{\alpha}(t) \\ &+ \sum_{i=1}^{n} \phi_i(L) \left[M\ddot{y}_i(t) + c\dot{y}_i(t) + ky_i(t)\right] + M\ddot{\alpha}(t) + c\dot{\alpha}(t) + k\alpha(t) = 0, \end{aligned} \tag{22}$$

where

$$\bar{\phi}_0 = \int_0^L (\frac{x}{L})^m dx. \tag{23}$$

Substituting Eq. (21) into Eq. (22), we transform Eq. (22) into

$$L\ddot{u}_r + \bar{\phi}_0\ddot{\alpha}(t) - m(m-1)/c_p^2\hat{\phi}_0\alpha(t) = 0, \tag{24}$$

where

$$\hat{\phi}_0 = \int_0^L \frac{x^{m-2}}{L^m}dx. \tag{25}$$

Substitution of Eqs. (17) - (19) into Eq. (10) yields

$$\begin{aligned} &\sum_{i=1}^{n} \phi_i(x) \left[\omega_i^2 y_i(t) + \ddot{y}_i(t)\right] + \ddot{u}_r(t) \\ &- m(m-1)\frac{c_p^2}{L^m}x^{m-2}\alpha(t) + (\frac{x}{L})^m\ddot{\alpha}(t) = 0, \end{aligned} \tag{26}$$

where $\omega_i = c_p\kappa_i$ and $\kappa_i = i\pi/L$. Multiplying Eq. (26) by $\phi_i(x)$ and integrating the equation over the length of the rod yields

$$\ddot{y}_i(t)+\omega_i^2 y_i(t)-m(m-1)c_p^2\hat{\phi}_i\alpha(t)+\bar{\phi}_i\ddot{\alpha}(t)=0, \tag{27}$$

where

$$\bar{\phi}_i=\int_0^L (\frac{x}{L})^m\phi_i(x)dx, \tag{28}$$

$$\hat{\phi}_i=\int_0^L \frac{x^{m-2}}{L^m}\phi_i(x)dx, \tag{29}$$

with $i=1,2,\cdots,n$.

The left boundary condition is automatically satisfied. Now, we transform the equations of motion (1) and (2) into a set of ordinary differential equations (ODEs) defined through Eqs. (21), (24) and (27). To solve for the set of ODEs, we define a vector of generalized coordinates

$$\mathbf{z}=[\alpha,u_r,y_1,\cdots,y_n]^T. \tag{30}$$

Eqs. (21), (24) and (27) can be rewritten in the matrix form as

$$\mathbf{M}\ddot{\mathbf{z}}+\mathbf{C}\dot{\mathbf{z}}+\mathbf{K}\mathbf{z}=0, \tag{31}$$

where

$$\begin{aligned}\mathbf{M}&=\begin{bmatrix} M & M\boldsymbol{\phi}(L)^T\\ \bar{\boldsymbol{\phi}} & \mathbf{L}\end{bmatrix},\mathbf{C}=\begin{bmatrix} c & c\boldsymbol{\phi}(L)^T\\ \mathbf{0} & \mathbf{0}\end{bmatrix},\\ \mathbf{K}&=\begin{bmatrix} k+EAm/L & k\boldsymbol{\phi}(L)^T\\ -m(m-1)c_p^2\hat{\boldsymbol{\phi}} & \boldsymbol{\omega}\end{bmatrix},\end{aligned} \tag{32}$$

and

$$\boldsymbol{\phi}(L)=[1,\phi_1(L),\phi_2(L),\cdots,\phi_n(L)]^T, \tag{33}$$

$$\bar{\boldsymbol{\phi}}=[\bar{\phi}_0,\bar{\phi}_1,\bar{\phi}_2,\cdots,\bar{\phi}_n]^T, \tag{34}$$

$$\hat{\boldsymbol{\phi}}=[\hat{\phi}_0,\hat{\phi}_1,\hat{\phi}_2,\cdots,\hat{\phi}_n]^T, \tag{35}$$

$$\boldsymbol{\omega}=diag(0,\omega_1^2,\omega_2^2,\cdots,\omega_n^2), \tag{36}$$

$$\mathbf{L}=diag(L,1,1,\cdots,1). \tag{37}$$

Define the state vector $\mathbf{Z}=[\mathbf{z},\dot{\mathbf{z}}]^T$. The state-space representation of Eq. (31) reads

$$\dot{\mathbf{Z}}=\mathbf{A}\mathbf{Z}, \tag{38}$$

where

$$\mathbf{A}=\begin{bmatrix} \mathbf{0} & \mathbf{I}\\ -\mathbf{M}^{-1}\mathbf{K} & -\mathbf{M}^{-1}\mathbf{C}\end{bmatrix}. \tag{39}$$

The formal solution of Eq. (38) reads

$$\mathbf{Z}(t)=e^{\mathbf{A}t}\mathbf{Z}_0, \tag{40}$$

where $\mathbf{Z}_0$ is the initial condition.

3.1 Initial condition $\mathbf{Z}_0$

Substitution of Eqs. (17) - (19) into the initial conditions in Eqs. (9) - (12) yields

$$\rho AL\dot{u}_{r0}+M\dot{u}_{r0}=f_0, \tag{41}$$

$$\dot{u}_{r0}+\sum_{i=1}^{n}\phi_i(0)\dot{y}_{i0}=\frac{f_0}{\rho A}, \tag{42}$$

$$u_{r0}+\sum_{i=1}^{n}y_{i0}+(\frac{x}{L})^m\alpha_0=0,\ 0\le x\le L, \tag{43}$$

$$\sum_{i=1}^{n}\phi_i(x)\dot{y}_{i0}+(\frac{x}{L})^m\dot{\alpha}_0=0,\ 0<x\le L, \tag{44}$$

where $u_{r0}=u_r(0)$, $\alpha_0=\alpha(0)$ and $y_{i0}=y_i(0)$. Because Eq. (43) holds for an arbitrary point on the rod, we obtain

$$u_{r0}=\alpha_0=y_{j0}=0,\ \ j=0,1,\cdots,n. \tag{45}$$

Hence, before impact, we have $\mathbf{z}_0=\mathbf{0}$.

Eq. (41) yields

$$\dot{u}_{r0}=f_0/(\rho AL+M). \tag{46}$$

Since we consider an impact excitation which can lead to numeric singularity, we propose a least squares solution. We uniformly sample $N-1$ points along the rod denoted as $x_k=kL/(N-1)$ for $k=1,2,\cdots,N-1$ and rewrite Eq. (44) as

$$\sum_{i=1}^{n}\phi_i(x_k)\dot{y}_i(0)+(\frac{x_k}{L})^m\dot{\alpha}(0)=0. \tag{47}$$

Let $\dot{\mathbf{z}}_0=[\dot{a}_0,\dot{y}_{10},\cdots,\dot{y}_{n0}]$. Using the least mean squares method for Eqs. (42) and (47), we obtain

$$\dot{\mathbf{z}}_0=(\mathbf{\Phi}^T\mathbf{\Phi})^{-1}\mathbf{\Phi}^T\mathbf{F}, \tag{48}$$

where $\mathbf{F}=[f_0/(\rho A)-\dot{u}_{r0},0,0,...0]^T$ and

$$\mathbf{\Phi}=\begin{bmatrix} 0 & \phi_1(0) & \phi_2(0) & \cdots & \phi_n(0) \\ (x_1/L)^m & \phi_1(x_1) & \phi_2(x_1) & \cdots & \phi_n(x_1) \\ \vdots & \vdots & \vdots & \ddots & \vdots \\ (L/L)^m & \phi_1(L) & \phi_2(L) & \cdots & \phi_n(L) \end{bmatrix}. \tag{49}$$

Hence, we completely determine the initial condition $\mathbf{Z}_0$ for Eq. (38).

4 Numerical examples

In this section, we will investigate the impact response of the rod with a mass-damper-spring termination in Fig.1 by making use of the analytical solution presented earlier. The response will be predicted with 200 elastic modes because it is sufficient to capture the dynamic response of the rod according to the numerical error analysis in Sec. 5. The displacement, velocity, and strain responses at selected locations on the rod will be studied. The impact loading applied at the free end produces the initial strain and velocity impulse. The rod response consists of two waves: the wave generated by the impact force at the left end and the reflected wave generated by the response at the right end. Because of the

Table 1 The parameters of the rod under investigated.

Parameter	Value	Parameter	Value
Young's Modulus, E, [Gpa]	10	Length, L, [m]	2
Mass, M, [kg]	0.5	Area, A, [m^2]	0.1
Stiffness, k, [N/m]	10	Damping, c, [Ns/m]	2
Density, ρ, [kg/m^3]	10	Impulse force, f_0, [N]	1

finite length of the rod, these two waves will be reflected back and forth leading to complex dynamical phenomena. The responses with traveling impulses at selected locations of the rod will be examined.

We also apply the proposed solution method to a rod with a viscous boundary condition. This problem has received much attention in past decades. Furthermore, the effect of the m-c-k termination on vibration modes of the rod will be discussed through the eigenvalue analysis of the state equation (38). We present the root loci of selected modes with respect to the mass, spring and damping coefficients, and numerically demonstrate the possibility to maximize the system damping with a proper choice of the mass-damper-spring termination.

4.1 Response with wave phenomenon

The parameters of the rod are listed in Table 1. Note that L/c_p is the time for the compressive stress wave to travel the length of the rod. Consider a normalized time defined by $\tau = t/(L/c_p)$. In the transient response analysis, we focus on the response over a time period when the compressive stress wave travels on the rod back and forth for the first three times. The transient impulse responses of the rod at $x = 0.25L$ and $x = L$ over this short time interval are shown in Fig.2.

The spikes in the velocity and strain responses at $\tau = 2.75$ and at various time instances $\tau = 0.25, 0.75, 1, 1.25, 1.75, 2, 2.75$ and 3 clearly indicate the arrival of the forward and reflected impulsive wave response to the initial impact at $x = 0$. Since the spikes are narrow in time, the displacement remains a smooth function of time. On the other hand, the strain response at $x = L$ shows impulsive spikes only at time instance $\tau = 1, 3, 5$ when the compressive stress wave reaches the end of the rod. Its velocity is less influenced by the compressive stress wave because of the large inertial of the m-c-k termination.

The displacement responses of the rod at $x = 0.25L$ and $x = L$ over a longer time span are presented in Fig.3. It should be noted that the internal damping of the rod is neglected. The responses decay due to the damping in the m-c-k termination at $x = L$.

4.2 Response with a viscous boundary condition

When only a damper is mounted to the right end, the eigenvalue problem becomes non-self-adjoint. This problem has been studied extensively in the literature. To the authors' best knowledge, the impulse response of such a problem has not been well studied. Here, we study the impulse response of the rod with a damper and very small mass at $x = L$, subject to an impact loading at $x = 0$. The parameters of the rod are the same as those in Table 1. The parameters for the m-c-k termination are $c = 2$ Ns/m and $k = 0$ N/m. The different values of the mass M are considered in the numerical studies.

Fig.4 shows the strain and velocity responses at the right end of the rod over a short time span. It can be seen from the figure that the impulse arrives at the right end when τ is an integer, as is the case in the earlier example. The velocity remains constant between impulses indicating that the damping force balances the internal elastic force at the right end. The strength of the impulses decreases quickly when the wave travels on the rod due to the damping at the right end. As the mass decreases, the response to the impulse at $x = L$ becomes quicker with sharper peaks. We should point out that as $M \to 0$, the response of the system converges to that of the rod with only a damper at the right end.

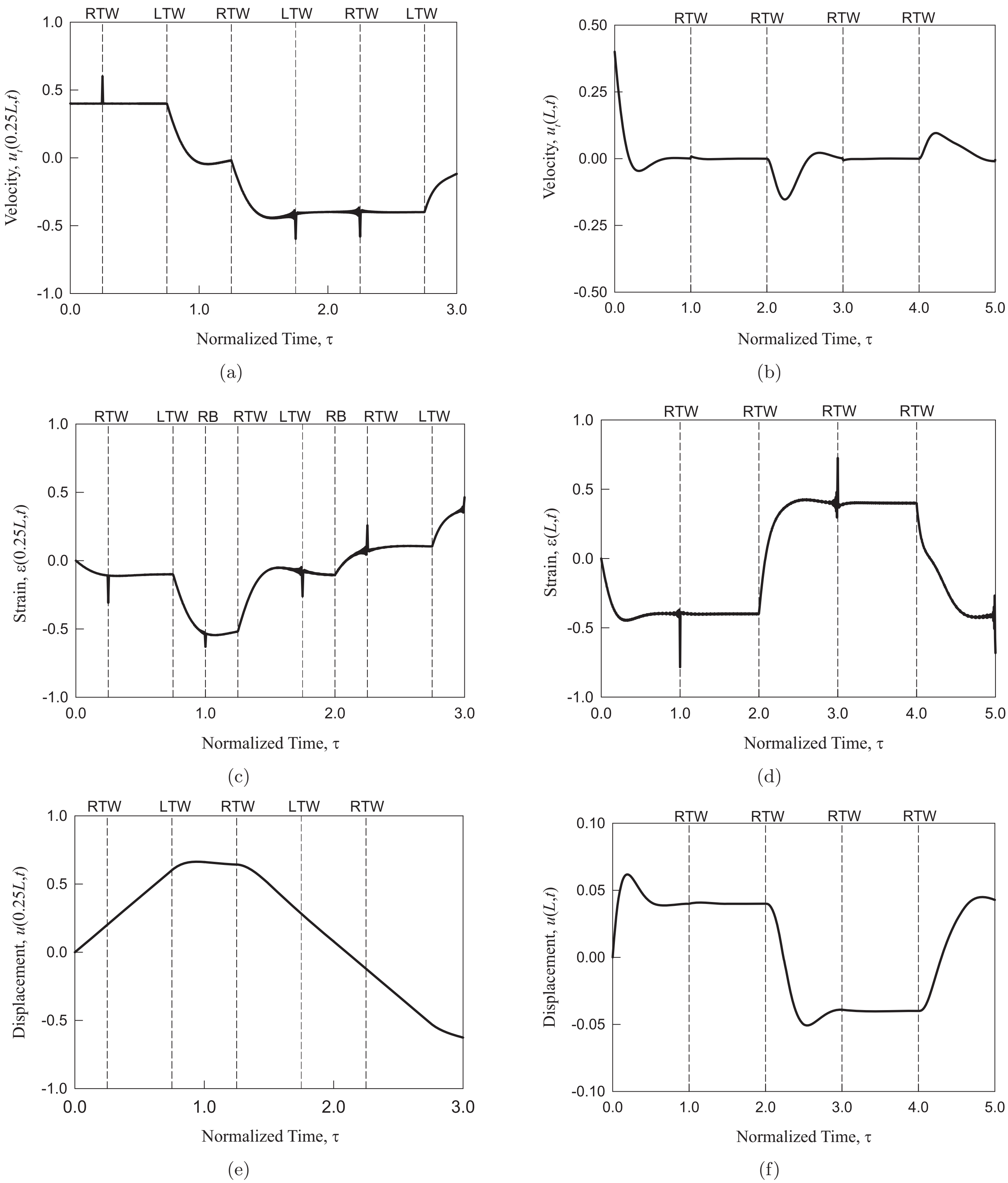

Fig. 2 The transient response of the rod at $x = 0.25L$ (Left column: (a), (c), (e)) and $x = L$ (Right column: (b), (d), (f)). Top row: Velocity. Middle row: Strain. Bottom row: Displacement. LTW: left traveling wave. RTW: right traveling wave. RB: the time instants when a wave reaches to the right boundary. $\tau = t/(L/c_p)$. $n = 200$.

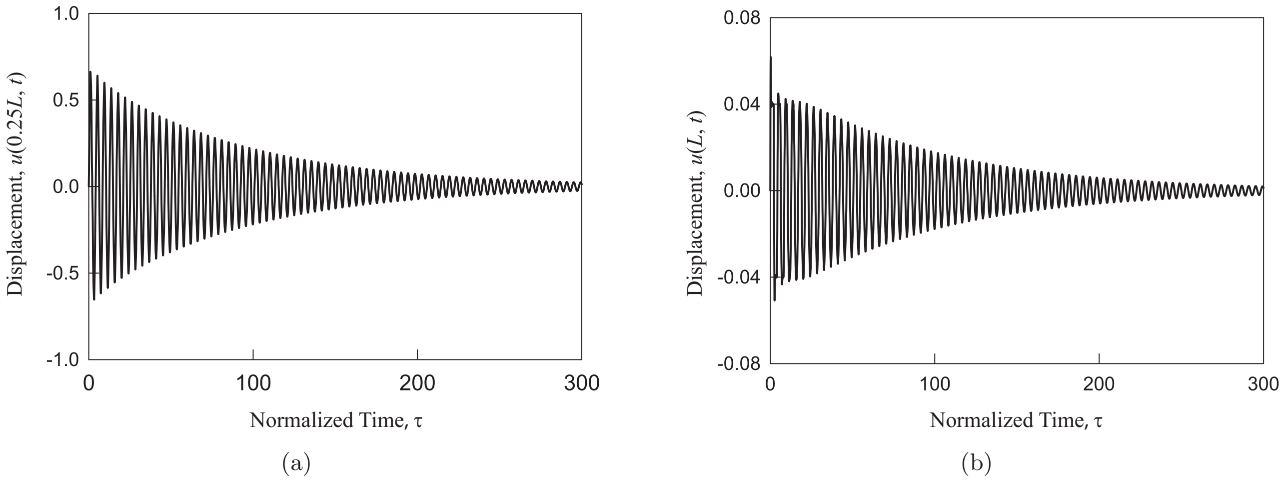

Fig. 3 The displacement response of the rod over a longer time span at (a) $x = 0.25L$ and (b) $x = L$. $n = 200$.

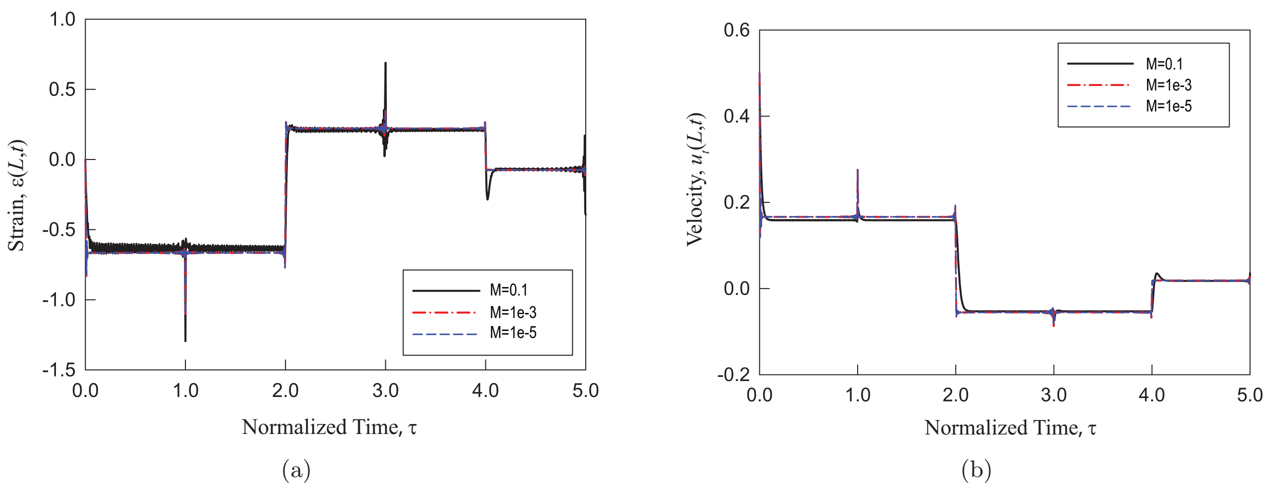

Fig. 4 The impact response of the rod with a damped boundary condition. $n = 200$.

4.3 Vibration reduction with termination design

It is understood that the m-c-k parameter values of the termination can change the vibration response of the rod. One way to reveal their effects on the vibration response is to examine the eigenvalues of the system. To this end, the root locus in control theory provides a handy tool [39]. Fig.5 shows the root loci of the rod with respect to one of the three m-c-k parameters while the other two are fixed. The m-c-k parameters and their ranges for each subplot of Fig.5 are listed in Table 2. Only the second quadrant of the root locus is shown because it is symmetrical with respect to the real axis and the real part of the eigenvalues is not positive.

As shown in Fig.5, the m-c-k termination has little influence on the eigenvalue associated with the particular solution. It, however, significantly affects on the eigenvalues of the rigid-body mode. By tuning the termination conditions, one can achieve underdamped, critically damped, and overdamped response of the rigid-body motion. The change of rigid-body-mode eigenvalues will lead to different couplings between the rigid-body and elastic modes. For example, with the increase of stiffness k in Fig.5(c), the dominant coupling with the rigid-body mode will be transferred from the first elastic mode

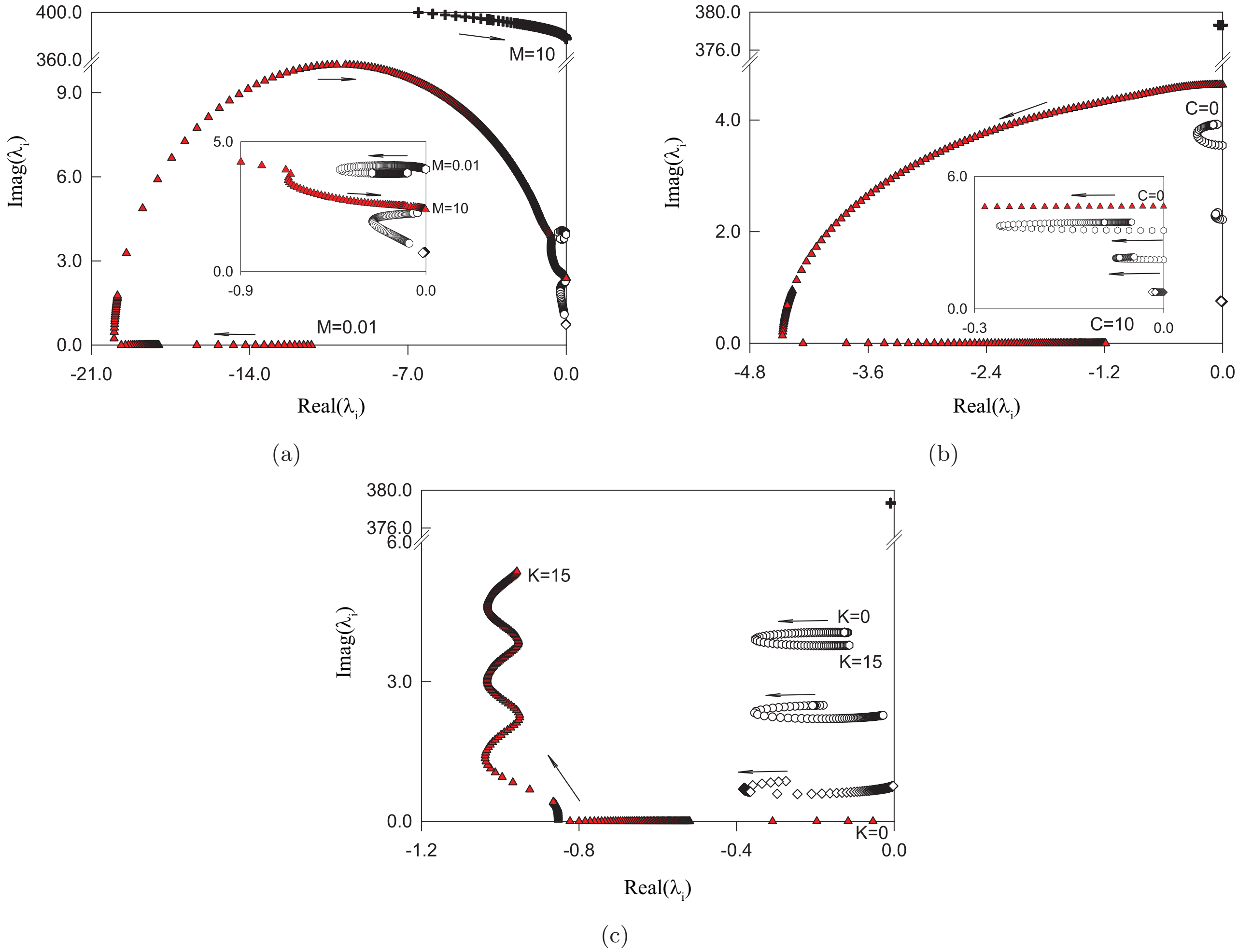

Fig. 5 The root locus of the lower order dominate modes of the rod with respect to the m-c-k parameters. (a) with respect to mass M. (b) with respect to damping c. (c) with respect to stiffness k. +: Particular solution. △: Rigid-body mode. ◇: The 1st elastic mode. ○: The 2nd elastic mode. ⬡: The 3rd elastic mode. $n=200$.

Table 2 The parameter settings for the root loci in Fig.5.

Subplot	Variable	Range	Fixed Parameters
(a)	M	(0.01, 10)	$k=10$, $c=2$
(b)	c	(0, 10)	$M=0.5$, $c=10$
(c)	k	(0, 15)	$M=0.5$, $c=2$

to the second mode, and so on. There exists a turning point on the root locus of every elastic mode. At the turning point, the coupling between the elastic mode and the rigid-body mode becomes strongest, leading to the smallest real part of the eigenvalue of the elastic mode. This property might be used to maximize the decay rate of the response of the elastic modes. Fig.5 also suggests that there exist finite ranges of m-c-k parameter values such that the largest damping for the system is achieved. The responses of the rod at $x=L$ and $x=1/4L$ as shown in Fig.6 indeed confirm that the vibration reduction of the rod by means of the termination design is achievable. Further studies on how to optimize the termination design will be reported in a separate work.

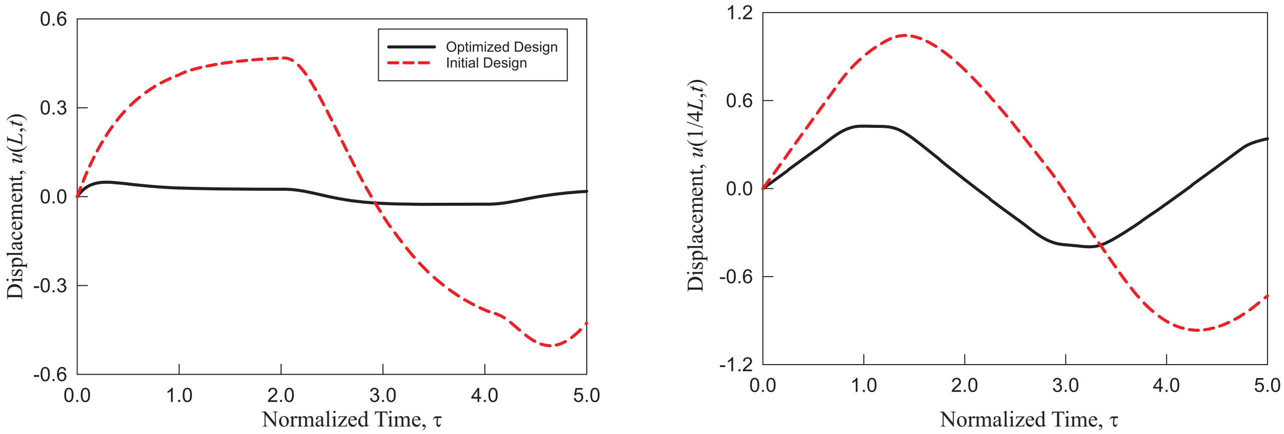

(a) (b)

Fig. 6 The rod vibration at $x = L$ and $x = 1/4L$ with different m-c-k terminations. Red dashed line: Initial termination design with $M = 0.1$, $c = 0.1$ and $k = 1$. Black solid line: Better design with $M = 2$, $c = 8$ and $k = 10$.

5 Error analysis

In this section, we investigate the accuracy and convergence of the proposed particular solution method. We first study the accuracy of the proposed solution by examining the error of the governing partial differential equation when the proposed solution is applied to the equation. This is a common practice to investigate the accuracy of approximate solutions when the exact solution or a highly reliable numerical solution does not exist for comparison. Recall that the particular solution method guarantees the satisfaction of all the boundary conditions. Hence, there is no boundary error to consider in this study. Next, we compare the proposed solution with the existing analytical solution for a rod with free-free boundary conditions.

5.1 Mean absolute error

We define an equation error for the rod in the domain $0 \leq x \leq L$, and for the concentrated mass at $x = L$ when the computed solution is applied to the equations of motion.

$$e_x(x,t,n) = \frac{E}{\rho}\frac{\partial^2 u_e}{\partial x^2} - (\ddot{u}_r + \frac{\partial^2 u_e}{\partial t^2}), \quad 0 \leq x \leq L \tag{50}$$

$$\begin{aligned} e_L(t,n) = {} & EA\frac{\partial u_e}{\partial x}(L,t) + M(\ddot{u}_r + \frac{\partial^2 u_e}{\partial t^2}(L,t)) \\ & + c(\dot{u}_r + \frac{\partial u_e}{\partial t}(L,t)) + k(u_r + u_e(L,t)), \end{aligned} \tag{51}$$

where n is the number of elastic modes included in the solution. Recall that the proposed particular solution method incurs zero error at the boundaries. We define the following mean absolute error as a measure of accuracy of the solution obtained with the proposed method.

$$e(n) = \frac{1}{T_f L}\int_0^L \int_0^{T_f} |e_x(x,t,n))| dt dx + \frac{1}{T_f}\int_0^{T_f} |e_L(t,n)| dt \tag{52}$$

where $T_f \gg 1$ is a time that is sufficiently large. We have taken $T_f = 10$ seconds in the numerical examples.

Fig.7 shows the mean absolute error $e(n)$ as a function of n. The spatial integration of the mean absolute error is computed by discretizing the rod evenly into 500 segments. The mean absolute error

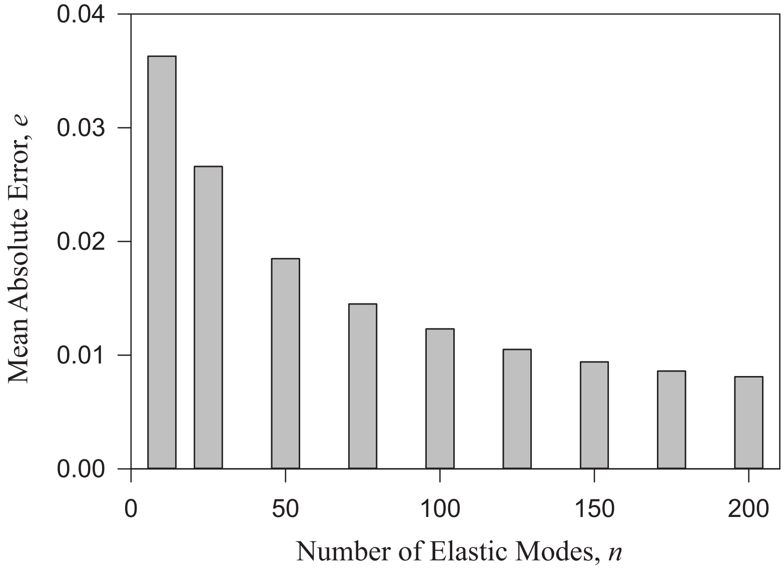

Fig. 7 Variation of the mean absolute error of the solution computed by the proposed method with the number of elastic modes.

Table 3 Comparison of frequencies of the rod obtained by the proposed particular solution (PS) method with the exact frequencies of the free-free rod. Frequency unit is radian per second. The zeroth order mode of the free-free rod is the rigid body motion with zero frequency.

Mode No. i	ω_i by PS Method	Exact ω_i
0	0	0
1	1.5708	1.5708
2	3.1416	3.1416
3	4.712	4.712
4	6.2832	6.2832
5	7.8540	7.8540
200	314.16	314.16

drops monotonically as n increases, down from $e(n) = 3.67 \times 10^{-2}$ with $n = 10$ to $e(n) = 7.875 \times 10^{-3}$ with $n = 200$. The convergence rate is relatively slow because the impulse response of strain and velocity of the rod is not smooth and its approximation requires very fine resolution both in time and space.

5.2 A free-free rod

Next, we validate the particular solution method with an extreme case when only a tiny mass is attached to the right end. This system is then close to the problem with free-free boundary conditions whose exact solution is known. The rod parameters are the same as in Table 1 except for $M = 1 \times 10^{-8}$ and $k = c = 0$.

The resonant frequencies of the system obtained by the particular solution method and those of the free-free rod are listed in Table 3. The exact frequency of the free-free rod is

$$\omega_i = \frac{n\pi}{l}, \tag{53}$$

with $i = 0, 1, 2, \ldots$. The frequencies for the rigid-body and elastic motions of the rod by the particular solution method are identical to their exact counterparts. The frequency associated with the particular

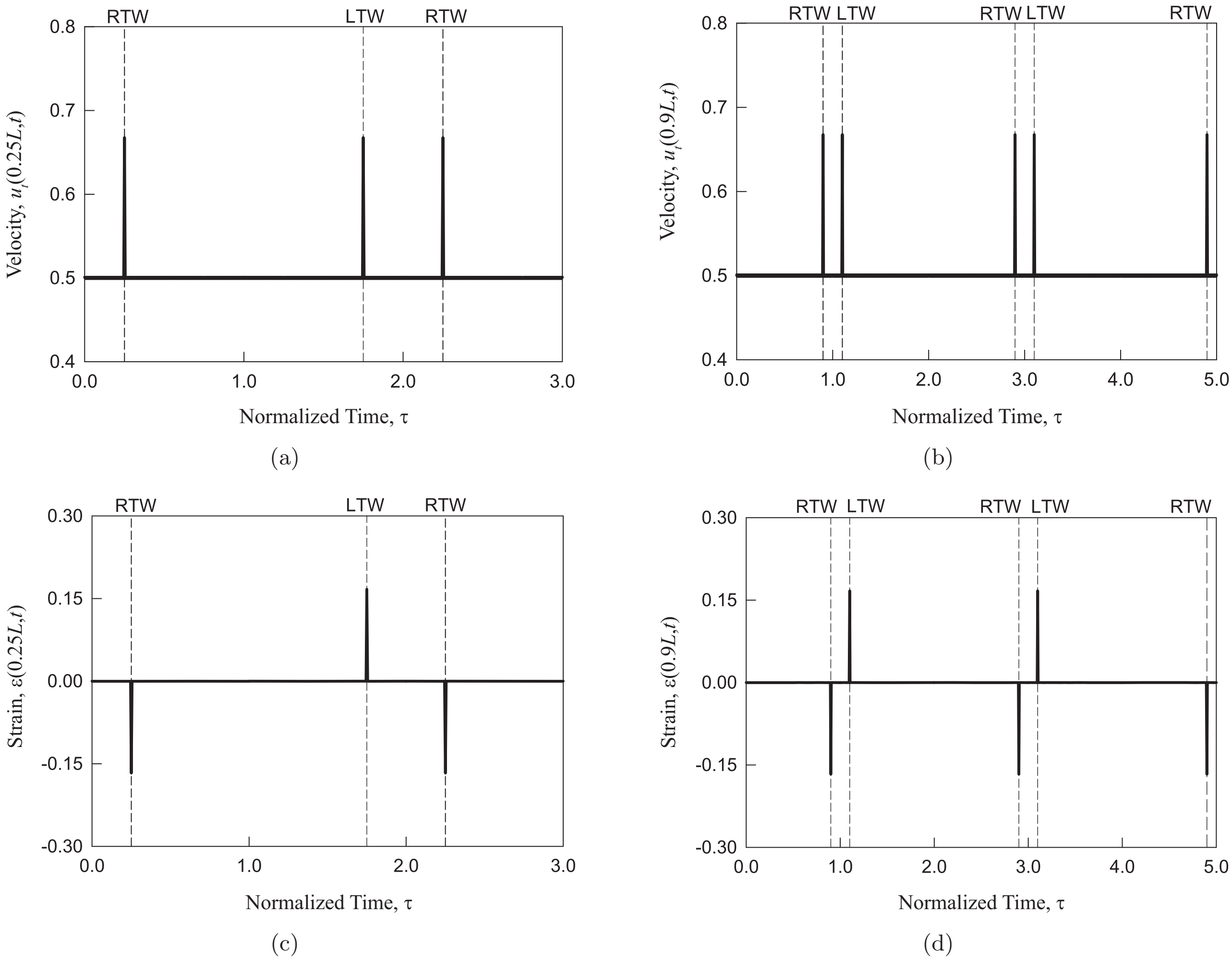

Fig. 8 The impulse response of the rod with almost free-free boundary conditions at $x = 0.25L$ (Left column (a) (c)) and at $x = L$ (Right column (b) (d)). Top row: Velocity. Bottom row: Strain. $n = 200$.

solution $\alpha(t)$ is 222420 radian per second, 707 times larger than the frequency of the 200th elastic mode. Such a high frequency is due to the extremely small mass $M = 1 \times 10^{-8}$. Its influence on the rod dynamics is thus negligible.

The responses of the rod at $x = 0.25L$ and $x = 0.9L$ are presented in Fig.8. Because of the free-free boundary conditions, between the arrival of impulses, the speed and strain of the rod remain constant. Sharp changes of the velocity and strain occur when a left or right traveling impulse arrives. It is clear that the dynamics of the impulse response with free-free boundary conditions is perfectly captured by the proposed particular solution method.

6 Conclusions

In this paper, we have investigated the impulse response of an elastic rod with a mass-damper-spring termination. Because the mass-damper-spring termination leads to a non-self-adjoint eigenvalue problem, we have solved this problem by using a particular solution method that constructs the solution of the system as the combination of a solution satisfying homogeneous boundary conditions and a particular solution to satisfy the nonhomogenous boundary conditions. The advantage of this approach is that the particular solution can satisfy nonhomogenous boundary conditions exactly, and transform the problem into a self-adjoint boundary value problem for the homogeneous part of the elastic response. The transient and total impulse responses of the rod have been studied in detail. The vibration reduction of the rod by tuning termination conditions has been discussed with the help of root locus. It has been showed that the termination can change the coupling between the rigid-body and elastic modes which affects the vibration of the rod. The particular solution method has also been validated through the error analysis and a comparison study of the vibration problem of a free-free rod.

Appendix

Initial conditions with impact loading

Consider an impact loading $f(x,t) = f_0\delta(t) + \varepsilon f_0\delta(x)\delta(t)$ applied to both the rigid-body and elastic motion. Herein, ε is an infinitesimal number used to remove the singularity due to the delta functions as $t \to 0$ and $x \to 0$. The equations of motion read

$$\begin{aligned}&\rho AL\ddot{u}_r + M\ddot{u}_r + c\dot{u}_r + ku_r + \rho A\int_0^L \frac{\partial^2 u_e(x,t)}{\partial t^2}dx\\&+ M\ddot{u}_e(L,t) + c\dot{u}_e(L,t) + ku_e(L,t) = f_0\delta(t),\end{aligned} \tag{A1}$$

$$c_p^2\frac{\partial^2 u_e}{\partial x^2} + \varepsilon\frac{1}{\rho A}f_0\delta(x)\delta(t) = \ddot{u}_r + \frac{\partial^2 u_e}{\partial t^2}. \tag{A2}$$

Integrating (A1) with respect to t from 0^- to 0^+, we obtain

$$\rho AL\dot{u}_r(0) + \rho A\int_0^L \frac{\partial u_e}{\partial t}(x,0)dx + M\left(\dot{u}_r(0) + \dot{u}_e(L,0)\right) = f_0, \tag{A3}$$

where we use the fact that the system is static before the impact. Integrating (A2) with respect to x from 0 to ε yields

$$c_p^2\frac{\partial u_e}{\partial x}(\varepsilon,t) + \frac{1}{\rho A}\varepsilon f_0\delta(t)\int_0^\epsilon \delta(x)dx = \ddot{u}_r\varepsilon + \frac{\partial^2 u}{\partial t^2}(\varepsilon/2,t)\varepsilon, \tag{A4}$$

where we use the mean-value theorem to evaluate the following integral

$$\int_0^\varepsilon \frac{\partial^2 u_e}{\partial t^2}dx = \frac{\partial^2 u_e}{\partial t^2}(\varepsilon/2,t)\varepsilon. \tag{A5}$$

Integrating (A4) with respect to t from 0 to ε yields

$$c_p^2\frac{\partial u_e}{\partial x}(\varepsilon,\varepsilon/2)\varepsilon + \frac{1}{\rho A}\varepsilon f_0 = \dot{u}_r(\varepsilon)\varepsilon + \frac{\partial u_e}{\partial t}(\varepsilon/2,\epsilon)\varepsilon. \tag{A6}$$

Taking the limit $\varepsilon \to 0$, we obtain

$$c_p^2\frac{\partial u_e}{\partial x}(0,0) + \frac{1}{\rho A}f_0 = \dot{u}_r(0) + \frac{\partial u_e}{\partial t}(0,0). \tag{A7}$$

In summary, the initial conditions with impact loading read

$$\rho AL\dot{u}_r(0) + \rho A\int_0^L \frac{\partial u_e}{\partial t}(x,0)dx + M\left(\dot{u}_r(0) + \dot{u}_e(L,0)\right) = f_0, \tag{A8}$$

$$c_p^2 \frac{\partial u_e}{\partial x}(0,0) + \frac{1}{\rho A} f_0 = \dot{u}_r(0) + \frac{\partial u_e}{\partial t}(0,0), \tag{A9}$$

$$u_r(0) + u_e(x,0) = 0, \text{ for } 0 \le x \le L, \tag{A10}$$

$$\frac{\partial u_e}{\partial t}(x,0) = 0, \text{ for } 0 < x \le L. \tag{A11}$$

References

[1] Feng, Q. and Shinozuka, M. (1993), Control of seismic response of structures using variable dampers, *Journal of Intelligent Material Systems and Structures*, **4**, 117-122.

[2] Jayachandran, V. and Sun, J.Q. (1998), Impedance characteristics of active interior noise control systems, *Journal of Sound and Vibration*, **211**, 716-727.

[3] Udwadia, F.E. (2005), Boundary Control, quiet boundaries, super-stability and super-instability, *Applied Mathematics and Computation*, **164**(1), 327-349.

[4] Spiekermann, C.E. and Radcliffe, C.J., (1988), Decomposing one-dimensional acoustic pressure response into propagating and standing waves, *The Journal of the Acoustical Society of America*, **84**(4), 1536-1541.

[5] Singh, R., Lyons, W.M., and Prater, G.J., (1989), Complex eigensolution for longitudinally vibration bars with a viscously damped boundary, *Journal of Sound and Vibration*, **133**(2), 364-367.

[6] Prater, G.J. and Singh, R. (1990), Eigenproblem formulation, solution and interpretation for non-proportionally damped continuous beams, *Journal of Sound and Vibration*, **143**(1), 125-142.

[7] Gürgöze, M. (1998), On the eigenfrequencies of longitudinally vibrating rods carrying a tip mass and spring-mass in-span, *Journal of Sound and Vibration*, **216**, 295-308.

[8] Gürgöze, M. and Erol, H. (1999), On the eigencharacteristics of longitudinally vibrating rods carrying a tip mass and viscously damped spring-mass in-span, *Journal of Sound and Vibration*, **225**, 573-580.

[9] Yüksel, S., Gürgöze, M., and Erol, H. (2002), Continuous and discrete models for longitudinally vibrating elastic rods viscously damped in-span, *Journal of Sound and Vibration*, **257**, 996-1006.

[10] Hull, A.J., Radcliffe, C.J., Miklavčič, M., and Maccluer, C.R. (1990), State space representation of the nonself-adjoint acoustic duct system, *Journal of Vibration and Acoustics*, **112**, 483-488.

[11] Hull, A.J. (1994), A closed form solution of a longitudinal bar with a viscous boundary condition, *Journal of Sound and Vibration*, **169**, 19-28.

[12] Jayachandran, V. and Sun, J.Q. (1999), The modal formulation and adaptive-passive control of the nonself-adjoint one-dimensional acoustic system with a mass-spring termination, *Journal of Applied Mechanics*, **66**, 242-249.

[13] Chrchill, R.V. (1942), Expansions in series of non-orthogonal functions, *Bulletin of the AMS*, **48**, 143-149.

[14] Morgan, G.W. (1953), Some remarks on a class of eigenvalue problems with special boundary conditions, *The Quarterly Journal of Mathematics*, **11**, 157-165.

[15] Walter, J. (1973), Regular eigenvalue problems with eigenvalue parameters in the boundary condition, *Mathematische Zeitschrift*, **133**, 301-312.

[16] Schneider, A. (1974), A note on eigenvalue problems with eigenparameter in the boundary conditions, *Mathematische Zeitschrift*, **136**, 163-167.

[17] Fulton, C.T. (1977), Two-point boundary value problems with eigenvalue parameter contained in the boundary conditions, *Proceedings of the Royal Society of Edinburgh Section A*, **77A**, 293-308.

[18] Hilton, D.B. (1979), An expansion theorem for an eigenvalue problem with eigenvalue parameter in the boundary condition, *The Quarterly Journal of Mathematics*, **30**, 33-42.

[19] Yang, B. (1996), Integral formulas for nonself-adjoint distributed dynamic systems,*AIAA Journal*, **34**(10), 2132-2139.

[20] Yang, B. and Wu, X. (1997), Transient response of one-dimensional distributed systems: a closed form eigenfunction expansion realization, *Journal of Sound and Vibration*, **208**, 763-776.

[21] Oliveto, G., Santini, A., and Tripodi, E. (1997), Complex modal analysis of a flexural vibrating beam with viscous end conditions, *Journal of Sound and Vibration*, **200**, 327-345.

[22] Svedholm, C., Zangeneh, A., Pacoste, C., François, S., and Karoumi, R. (2016), Vibration of damped uniform beams with general end conditions under moving loads, *Engineering Structures*, **126**, 40-52.

[23] Alati, N., Failla, G., and Santini, A. (2014), Complex model analysis of rods with viscous damping devices, *Journal of Sound and Vibration*, **333**, 2130-2163.

[24] Sorrentino, S., Marchesiello, S., and Piombo, B.A.D. (2003), A new analytical technique for vibration analysis of non-proportionally damped beams, *Journal of Sound and Vibration*, **265**, 765-782.

[25] Sorrentinoa, S., Fasanab, A., and Marchesiellob, S. (2004), Frequency domain analysis of continuous systems with viscous generalized damping, *Shock and Vibration*, **11**, 243-259.

[26] Jovanovic, V., (2012), A Fourier series solution for the longitudinal vibrations of a bar with viscous boundary conditions at each end, *Journal of Engineering Mathematic*, **79**, 125-142.
[27] Jovanovic, V. and Koshkin, S. (2011), Explicit solution for vibrating bar with viscous boundaries and internal damper, *Journal of Engineering Mathematics*, **76**, 101-121.
[28] Failla, G. (2016), An exact generalised function approach to frequency response analysis of beams and plane frames with the inclusion of viscoelastic damping, *Journal of Sound and Vibration*, **360**, 171-202.
[29] Ülker-Kaustell, M., Karoumi, R., and Pacoste, C. (2010), Simplified analysis of the dynamic soil-structure interaction of a portal frame railway bridge, *Engineering Structures*, **32**, 3692-3698.
[30] Doménech, A., Martínez-Rodrigo, M.D., Romero, A., and Galvín, P. (2015), Soil–structure interaction effects on the resonant response of railway bridges under high-speed traffic, *International Journal of Rail Transportation*, **3**, 201-214.
[31] Hirzinger, B., Adam, C., and Salcher, P. (2020), Dynamic response of a non-classically damped beam with general boundary conditions subjected to a moving mass-spring-damper system, *International Journal of Mechanical Sciences*, **185**, 105877 (14 pages).
[32] König, P., Salcher, P., Adam, C., and Hirzinger, B. (2021), Dynamic analysis of railway bridges exposed to high-speed trains considering the vehicle-track-bridge-soil interaction, *Acta Mechanica*, **232**, 4583-4608.
[33] König, P., Salcher, P., and Adam, C. (2022), An efficient model for the dynamic vehicle-track-bridge-soil interaction system, *Engineering Structures*, **253**, 113769 (15 pages).
[34] Zangeneh, A., Museros, P., Pacoste, C., and Karoumi, R. (2021), Free vibration of viscoelastically supported beam bridges under moving loads: Closed-form formula for maximum resonant response, *Engineering Structures*, **244**, 112759 (11 pages).
[35] Qiao, G. and Rahmatalla, S. (2021), Dynamics of Euler-Bernoulli beams with unknown viscoelastic boundary conditions under a moving load, *Journal of Sound and Vibration*, **491**, 115771 (19 pages).
[36] Mao, X.Y., Sun, J.Q., Ding, H., and Chen, L.Q. (2020), An approximate method for one-dimensional structures with strong nonlinear and nonhomogenous boundary conditions, *Journal of Sound and Vibration*, **469**, 115128 (14 pages).
[37] Fahy, F. (1985), *Sound and Structural Vibration*, Academic Press: London.
[38] Meirovitch, L. (1967), *Analytical Methods in Vibrations*, The MacMillan Company: London.
[39] Franklin, G.F., Powell, J.D., and Emami-Naeini, A. (1994), *Feedback control of dynamic systems*, Pearson Education: New Jersey.